Heat Advection in the Active Layer of Permafrost: Physical Modelling to Quantify the Impact of Subsurface Flow on Soil…

Article · September 2015

CITATIONS
0

READS
129

5 authors, including:

Sabine Veuille
Université de Montréal
16 PUBLICATIONS **3** CITATIONS
SEE PROFILE

Daniel Fortier
Université de Montréal
248 PUBLICATIONS **761** CITATIONS
SEE PROFILE

Katerine Grandmont
Yukon College
28 PUBLICATIONS **12** CITATIONS
SEE PROFILE

Simon Charbonneau
Université de Montréal
6 PUBLICATIONS **5** CITATIONS
SEE PROFILE

Heat Advection in the Active Layer of Permafrost: Physical Modelling to Quantify the Impact of Subsurface Flow on Soil Thawing.

Sabine Veuille, Daniel Fortier, Manuel Verpaelst, Katerine Grandmont,
Geography Department, University of Montreal, Montreal, Quebec, Canada.
Centre for Northern Studies, Quebec, Quebec, Canada.
Charbonneau, Simon
Geography Department, University of Montreal, Montreal, Quebec, Canada.

ABSTRACT
To measure the impact of water flow on permafrost degradation, several experiments of active layer physical models were conducted in laboratory. Eight wooden cells filled with different quasi-saturated soils were subjected, for the first half, to a thawing by conduction and for the other half to a thawing by convection (water flow). The purpose of this protocol is to develop, with experimental data, tools to quantify the efficiency of thawing by conduction in comparison to thawing by convection.

RÉSUMÉ
Afin de mesurer l'impact des transferts de chaleur par écoulement d'eau sur la dégradation du pergélisol plusieurs expériences consistant à modéliser physiquement la couche active sont menées en laboratoire. Huit cellules de bois remplies de différents sols quasi-saturés sont soumises pour la moitié à un dégel favorisant la conduction et pour l'autre moitié à un dégel favorisant la convection par écoulement d'eau. L'approche proposée consiste à quantifier l'efficacité du dégel par conduction par rapport au dégel par convection à partir de ces données expérimentales.

1 INTRODUCTION

Warming of permafrost geosystems alters the active layer dynamics, essentially by increasing its thickness. Melting of ground ice in the upper portion of permafrost then triggers surface settlement, which changes the local topography and consequently the surface and subsurface flow paths.

Several studies have demonstrated that surface run-off as well as sub-surface water flow contribute to accelerate and increase active layer thawing (Kane 2001, Fortier 2007, Woo 2008, Jorgenson 2010, Rowling et al. 2011, de Grandpré et al. 2010, 2012), especially when the transient layer is ice-rich (Shur et al. 2005, Overduin and Kane 2006). Talik under rivers, deeper active layer under streams, rills and water tracks provide field examples of this process. In the active layer, subsurface water that flows through the soil porosity triggers convective heat transfer processes. On the opposite, if the water doesn't move, heat is transferred by conduction through the active layer. The efficiency of thawing by convective heat transfer compared to conductive heat transfer has often been reported but few studies have quantified it (Lunardini 1986). Quantifying the efficiency of thawing by convection versus conduction is complex. In the field, it is difficult to control all parameters and to separate physically, thus isolate mathematically, the two types of heat transfer.

Water temperature, flow rate and ground ice content are determining parameters, while ice temperatures have a negligible effect on the rate of ice ablation and permafrost degradation by convective heat flow (Lunardini 1986, Costard 2003, Randriamazaoro 2007). When the water temperature reaches its maximum, in most cases at the onset of convective transfer when water flow initiates, ice ablation is extremely rapid. The phenomenon is non-linear and quasi-exponential, and then gradually slows down. The more effective the convective transfer is, the more amplified is the thawing acceleration (Randriamazaoro 2007). Rates and magnitude of heat transfers are therefore particularly important during this period. In permafrost, if water drains off the sediment once the ice is melted, the ablation rate increases as the ice content decreases. (Dupeyrat 2011).

The fluid velocity, the heat transfer coefficient between the fluid and the solid it is in contact with, and the temperature differences between liquids and solids, are three basic parameters that determine convective heat transfers. When ice is involved, the heat transfer coefficient is particularly difficult to determine due to the interplay between temperature, materials, phase change and a moving boundary layer. Furthermore, convective heat transfers never occur alone and are always at least coupled with conductive heat transfers. Obtained after the non-dimensionalization of thermal equations, the Nusselt number is the ratio between both heat transfers and is thus difficult to assess (Chassaing 2010, Bianchi et al. 2004, Bear 1972). The Peclet number, which is the ratio between the convection transport rate, (through the forces of inertia) and the diffusion transport rate, is generally used to predict which of the two heat transfers is dominant (Chassaing 2010, Bianchi et al. 2004, Bear 1972). However, the Peclet number does not take into account the advection of latent heat released or stored during phase changes (Kane 2001). Also, the term of velocity included in the Peclet number (thermal or mass) is generally associated, in soil science, to the infiltration rate of a liquid in the soil (Huysmans, 2005). But because the velocity varies when the ground ice changes phase, the

Peclet number varies accordingly, making it difficult to use for the present study.

The objective of this work is to develop methodological tools to quantify the importance of convective heat transfer induced by water flow in the active layer and to determine at which point it becomes significant in comparison with conductive heat transfer.

Thawing time of frozen ground can be recorded by a temperature sensor and is easy to measure. This data indirectly contains information to assess the rate of ice ablation and allows to compare, if the experimental design is appropriate and subject to similar environmental conditions, different forms of heat transfers. From the *time* variable, it is also possible to calculate the thawing speed and by extension the heat propagation speed and total heat flux. The *time* variable thus indirectly encompasses the fluid velocity, ablation rate, coefficient of heat transfer and thermal conductivity while allowing distinguishing and measuring the efficiency of water flow-related heat transfer and air temperature-related heat transfer.

Experiments were carried out in a temperature-controlled room (environmental simulator) to replicate physical active layer of permafrost models and to compare under simulated changing “climatic conditions” (air water, soil temperature) the efficiency of the two heat transfer processes. This permitted to link laboratory tests to typical field conditions, under rigorous experimental conditions. 3D scans were made to visualise the displacement of material after thawing. Mathematical tools were also developed to quantify the efficiency of thawing by convection versus thawing by conduction (see section 3.2).

2 EXPERIMENTAL DESIGN

Eight wooden cells filled with frozen saturated soil were submitted to thawing in an environmental simulator (Figure 1). Four cells were thawed by air temperature only, while the other four were thawed by air temperature and flowing water. To avoid water stagnation, the cells were slightly inclined according to a 6° slope. To minimize side effects and ensure that water flowed in the middle of the cells, a shallow and narrow channel (1cm wide, 1 cm deep) was excavated into the soil of each cell for every test. Soil properties were measured and remained constant for each test (their values are presented in Tables 4 and 5). Tests were conducted four times to ensure that they were reproducible and statistically sound. These replicates also allowed to ensure that the intra-test variability (i.e., when the variables were similar) was not greater than or equal to the inter-test variability (i.e., when the variables were different). “Convective” and “conductive” tests were realized simultaneously in the environmental simulator, and were therefore subjected to the same ambient temperature conditions. The air temperature of the environmental simulator was recorded with thermistors during the tests to ensure that variations were minimal. For each test the air and water temperatures, the water flow, and the slope varied according to a predetermined protocol, and tests were made with sand and silt.

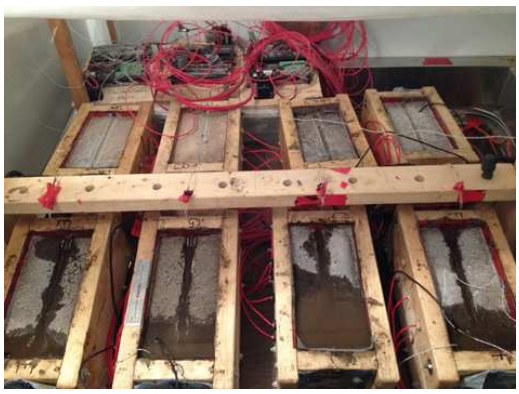

Figure 1. Eight thawing-cells during an experiment in a temperature-controlled environmental simulator.

2.1 Experimental Thawing-cells Description

Eight waterproof wooden cells 3.18 cm-thick with an internal volume of 7200 cm^3 were equipped with thermistor cables. The thermistors locations are presented in Table 1 and Figure 2.

Table 1. Thermistors locations. Distances are given relative to the upstream (x) surface (y) in cm.

Thermistor name	x	y
Top Upstream (TU)	7.7	2.7
Bottom Upstream (BU)	7.7	9.7
Center (C)	15.6	6.0
Top Downstream (TD)	23.6	2.7
Bottom Downstream (BD)	23.6	9.7

Thermistors were connected to a data logger (Campbell Scientific CR1000) and a multiplexer (Campbell Scientific AM16/32b) to record temperatures every five minutes.

Five holes (2 cm in diameter) located in the downstream wall of the cells allowed for water to drain by gravity. These holes were blocked to prevent drainage during preparation of the sample until complete freeze-back of the material.

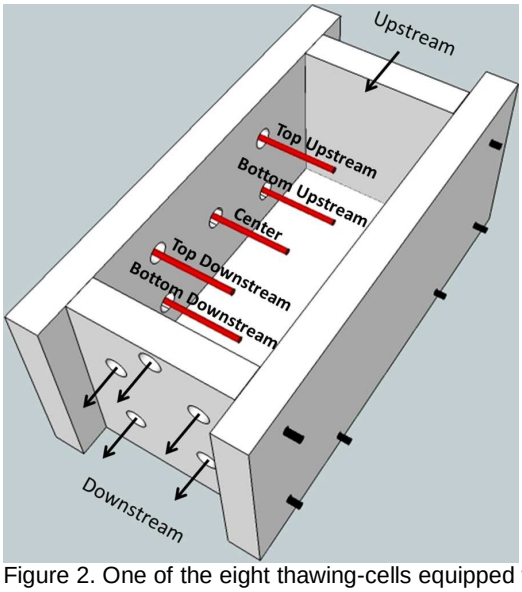

Figure 2. One of the eight thawing-cells equipped with five thermistors cables (red). Arrows indicates the direction of sub-surface flow out of the cell through holes.

2.2 Water Supply

Two 202L water tanks located "upstream" of the thawing-cells were maintained at a constant temperature using temperature-controlled, refrigerated, circulating baths (PolyScience 15L, Temperature stabilities ±0.005°C). Water contained in those two tanks was continuously pumped into two smaller containers located inside the tanks by using a submersible water pump. The overflow from these smaller containers was then returned to the bigger tanks, ensuring a constant pressure in the smaller containers. Water contained in the latter was then channelled by gravitational pressure to the convection cells via injection tubes (Baxter, model JC6401). A thermistor fixed at the mouth of the tube and connected to a data logger recorded the water temperatures. The flow rates were set manually before each test. Pressure loggers placed in the water tanks and in the air, allowed for validating (atmospheric pressure, that the flow rate was constant for the duration of the tests (Figure 3). By converting water pressure into water height, we continuously measured the water volume contained in both the tanks and containers. Using this data, we then calculated the water flow by using a linear relation between water volume and elapsed time.

2.3 Experimental Variables: Water and Air.

Multiple experimental scenarios were studied (Table 2). They looked at the difference between water (Tw) and air (Ta) temperatures. The tested temperatures were either 5°C (''cold'') or 15°C (''warm'')

The difference of temperature between water and air could therefore be -10°C (Tw=5°C - Ta=15°C), 0°C (Tw=15°C - Ta=15°C or Tw=5°C - Ta=5°C) and +10°C (Tw=15°C - Ta=5°C). The case Tw=5°C, Ta=5°C had already been studied during preliminary tests. Results were similar to the case Tw= 15°C, Ta=15°C but the time required to complete the test was longer. This case was therefore not considered (Fortier et al. 2014b).

The flow rates varied from 0.14 to 0.60 cm^3/s for each of these temperature differences (-10, 0, +10 °C) for the tests with sand and silt. Because of the geotechnical properties of silt, making the material difficult to be manipulated and homogenously saturated, sand was first used to validate the method. The slopes were maintained constant at 6° except for four tests made with sand, where the slope angles were set to 1°, 15° and 25°.

Table 2. Values of variables in experimentations

Tw - Ta	Flow	Slope	Material
(°C)	(cm^3/s)	(%)	
+10	0.13	6	Sand
+10	0.32	6	Sand
+10	0.45	6	Sand
+10	0.62	6	Sand
+10	0.62	6	Sand
0	0.14	6	Sand
0	0.62	6	Sand
-10	0.16	6	Sand
-10	0.21	6	Sand
-10	0.44	6	Sand
+10	0.15	1	Sand
+10	0.16	25	Sand
+10	0.17	15	Sand
+10	0.14	6	Silt
+10	0.32	6	Silt
+10	0.45	6	Silt
+10	0.65	6	Silt
0	0.62	6	Silt

2.4 Using 3D Laser Scanning to Visualize Material Displacement

To show and interpret the total displacement of the material after the tests, 3D laser scans of the soil surface were done using a Trimble® VX spatial station (single 3D point). Scans were made before and after the tests from one base station. The obtained point cloud was represented as a surface using a triangulated irregular network (TIN) method, using the Trimble® Realworks® 7.2 software.

A comparison analysis provided the settlement-accumulation measurements. Figure 4 shows how the material was redistributed downstream during a sand test, and provides information on how much displacement was produced, under a given slope angle, by the thawing of materials.

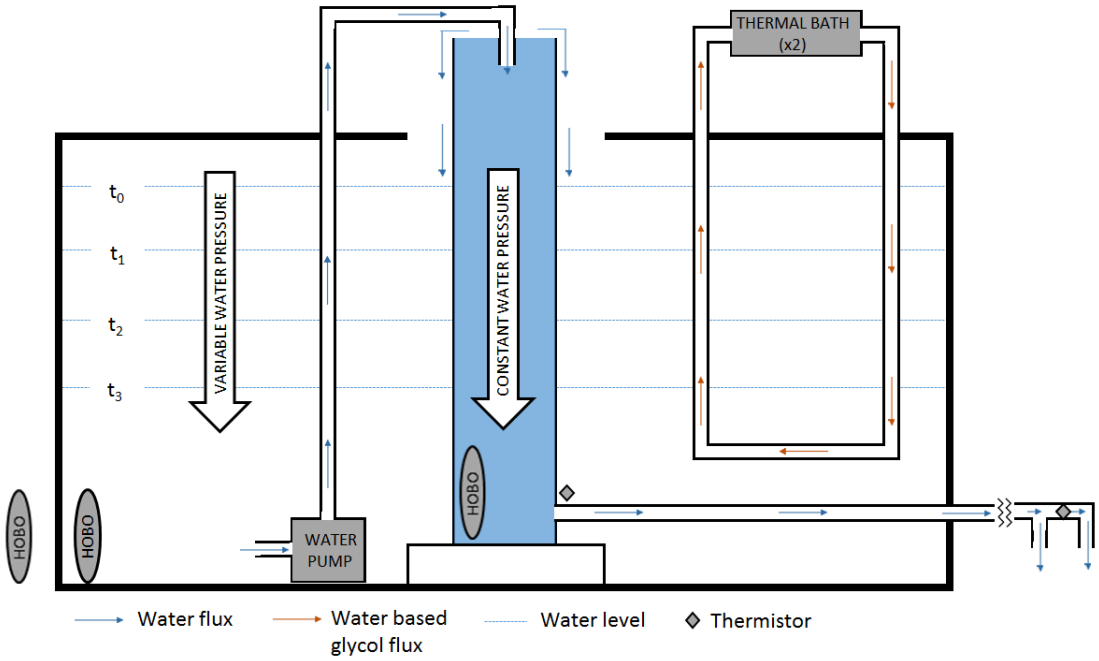

Figure 3. Schematic of water supply. “Hobo” is a pore-water pressure/water temperature sensor (Onset U20). The hobo outside of the water reservoir records barometric pressure used to correct water elevation measures.

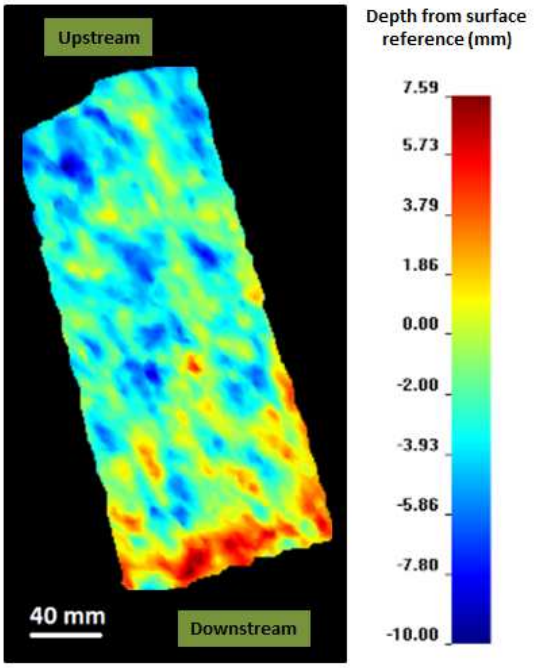

Figure 4. Surface comparison analysis. The image shows the differential mass movement of sand after completion of the test. As expected, settlement occurred mainly, but not exclusively, upstream while accumulation was highest downstream.

Table 3. Specification sensor details

Sensor	Type of measure	Cie	Data logger	Accuracy /Resolution
Thermistor NTC	Temperature	YSI	CR1000 AM16 32	0.10°C/ 0.001
TDR EC5	Water content	Decagon	Em50	±3%/0.1 VWC
Hobo U20	Pressure	Onset	Hobo Data Logger	±0.05% FS, 0.5/0.21 cm of water ±0.3% FS, 0.62/0.02 kPa
TP08	Thermal conductivity	Huksflux	CR1000	± (3% + 0.02)/NA W/mK
DSC	Heat capacity	TA Instrument	NA	3%/NA
Spatial Station VX	Scanning	Trimble	NA	1/0.43 cm

3. MATERIAL PROPERTIES

The degree of saturation and density of the saturated material were controlled to allow the comparison between different tests. To ensure the reproducibility of these parameters, a known quantity of material and water was poured in each cell to occupy a known volume. For tests

performed on sand, the material was oven dried before each test. Drying the silt is a long process where material has to be crushed each time. To bypass this step, each cell was initially weighted and once a test was completed, the cells were weighted again and the right amount of water was added to make up for the water loss that occurred during the test. To ensure a homogenous saturation and water content between the different cells, water content was measured by Time Domain reflectometry (TDR). TDR were placed downstream of each cell at 2 cm (top). The water content was measured and recorded every five minutes using a data logger (EM50, Decagon) during the experiments.

Particle size distribution was measured in the laboratory following a modified version of the ASTM D-422 protocol (ASTM 2007b), for sandy and silty materials respectively. All particles coarser than 2 mm and finer than 125 µm were removed from the sandy material. A 151-H hydrometer was used to measure the grain-size distribution of the silty material. Organic matter content was measured on 10 air-dried samples for both sandy and silty materials. Each sample was first weighted (m_b), then burned for 6 hours in an oven at 600°C, then weighted again (m_a). Mean organic matter content (*OMC*) was then calculated using the following equation:

$$OMC\ \% = \frac{1}{n} \times \left(\sum_{i=1}^{n} \frac{m_b - m_a}{m_b} \right) \times 100 \quad [1]$$

Where n is the total number of samples.

Table 4. Physical properties of tested soils

Geotechnical properties	Unit	Sand	Silt
Specific gravity	g/cm^3	2.70	2.58
Total volume	cm^3	5850	5850
Solid mass	g	9477	7697.43
Dry bulk density	g/cm^3	1.62	1.32
Porosity	%	40.0	49.0
Void ratio	%	66.7	96.1
Void volume	cm^3	2340.0	2866.5
Water volume	cm^3	1850.0	2665
Wet bulk density	g/cm^3	1.94	1.77
Volumetric water content	%	31.6	45.6
Gravimetric water content	%	19.5	34.6
Saturation	%	79.1	93

The specific gravity of the sediments was measured on 9 samples for both sandy and silty materials, following the ASTM C29-C29M protocol (ASTM 2007a). A mean specific gravity was then calculated for both materials.

The thermal conductivity of the soils at saturation was measured with a thermal conductivity probe (Hukseflux, TP08), and the heat capacity was measured using Differential Scanning Calorimetry (DSC) technology (Fortier et al. 2014a).These data will be compared to those extracted from the literature (Williams and Smith 1989, Andersland and Ladanyi 2004). Measurement results are presented in Table 5.

Table 5. Thermal properties of soils

Thermal properties	Sand		Silt	
	Saturated		Saturated	
	Frozen	Unfrozen	Frozen	Unfrozen
Thermal conductivity W/m/K	2.14	1.35	1.56	0.74
	Dry		Saturated	
			Frozen	Unfrozen
Heat capacity J/g/K	0,787		1.08	1.32

4. RESULTS AND DISCUSSION

At the air-soil interface for the first four cells, heat exchange was done by conduction into the soil. When the ice thawed, the water flowed by gravity. The soil in the cells was therefore also subjected, to a limited extent, to heat transfer by convection although the dominant heat transfer mechanism was clearly conductive. Indeed, in this case, the temperature difference between water and ice was small and the amount of water was negligible. To simplify the analysis, these cells were called "conduction cells".

For the other four cells submitted to water flow, heat exchanges were done by convection and by conduction into the soil. When the ice melted, the soil became permeable and flowing water, induced both by melting ice and upstream water, penetrated into the ground. The heat exchange was thus conducto-convectif. However heat transfers exchange was predominantly convective. To simplify, these cells were called "convection cells".

4.1 Thawing Time of Frozen Soils

We studied the thawing time of frozen soils. Graphically, thawing is easy to identify and is illustrated by the end of the zero curtain effect (van Everdingen, 1998) measured by thermistor readings within the cells (Figure 5).

Prior to the tests, the cells were put to freeze for 48 hours at a temperature of -19°C. Once frozen, they were relocated in the environmental simulator. The time between which the cells were taken out of the freezer and put in the environmental simulator can vary between each test, causing a slight difference in ice temperatures between the surface, the centre and the side-walls of the cells. However, it has been demonstrated that ice temperature doesn't have an important impact on the ablation rate (Lunardini 1986). It was arbitrarily determined that the start time for each test would be set when all thermistors indicate -16°C +/- 3°C. If this condition wasn't met before the start of the test, the test was invalidated.

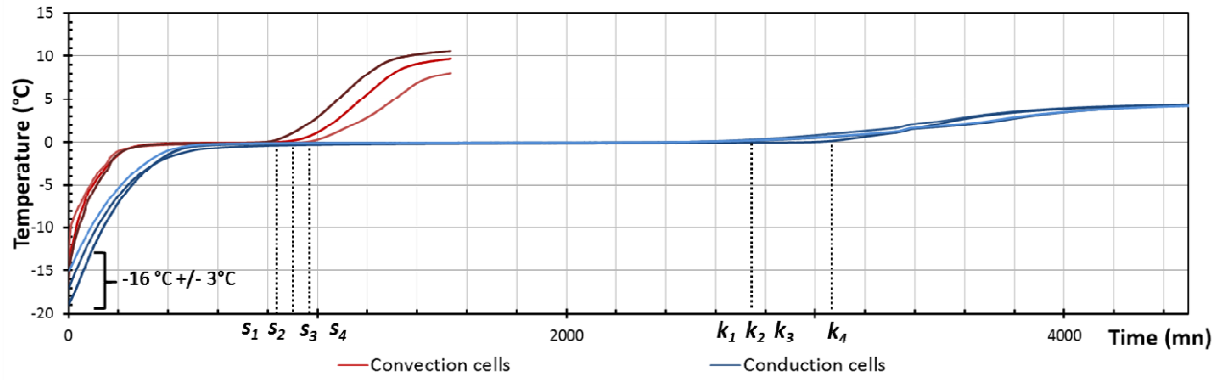

Figure 5. Example of initial condition and use of zero curtain effect to determine the thawing time. s_1, s_2, s_3, s_4 is the thawing time in the 4 convection cells and k_1, k_2, k_3, k_4 is the thawing time in the 4 conduction cells.

4.2 Effectiveness of Thawing by Convection vs Conduction

An efficacy index was developed to compare and quantify the effectiveness of thawing by convection against thawing by conduction. This index is the ratio between the thawing time calculated by a thermistor cable in a conduction cell and the thawing time calculated by a thermistor cable located at the same position in a convection cell. The equation is performed the same way with all the convection cells. A mean is then calculated with the 4 ratios. The same operation is then applied for the three other conduction cells. A second mean is finally calculated with these results. Equation [2] summarizes this method:

$$\varepsilon = \frac{1}{n}\sum_{i=1}^{n}\frac{1}{m}\sum_{j=1}^{m}\left(\frac{k_i}{s_j}\right) \qquad [2]$$

Where ε is the thawing efficiency of conduction versus convection, n and m are respectively the total number of cells in conduction and convection. k_i and s_j are respectively the thawing time for conduction and convection. In the case of these experiences, $n=m=4$.

When ε is greater than 1, the thawing time is greater in conduction cells than in convection cells. It is therefore admitted that for the same conditions of air temperature and slope for a given material, the heat transfers by convection are more efficient than the heat transfers by conduction. Inversely, when ε is lower than 1, the thawing time in conduction cells is lower than in convection cells. In this case and for the conditions of the test, the convective heat transfers are less efficient than the conductive heat transfer, which means that the thawing process is slowed by the convective heat exchanges. When $\varepsilon=1$, the thawing time is even for the cells in conduction and convection. It is important to note that the efficiency index does not measure the absolute efficacy of a heat process, it measures a ratio of two processes and thereupon the efficiency of one in comparison to the other.

Figure 6 shows the results of experiments that have been conducted during this research project. The thawing efficiency rate of conduction versus convection, for the central thermistor which is less influenced by side effects, as a function of the flow rate for 10 tests is presented below.

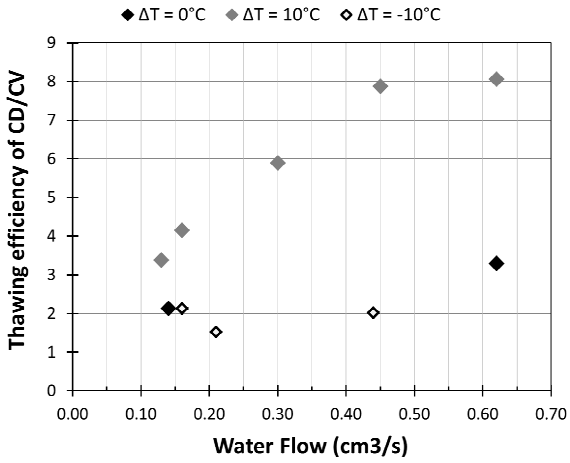

Figure 6. Thawing efficiency as a function of the flow for the sand.

When the temperature difference between water and air was positive or nil, the thawing efficiency rate of conduction versus convection increased with the flow rate. However the magnitude of this process was much greater when the temperature difference was positive. This means that when water temperature was higher than air temperature, the thawing efficiency was significantly amplified; for example, with a flow of 0.6 cm^3/s, the thawing efficiency was 2.5 times higher in comparison with the situation where both temperatures were equals. In this case, even if temperatures were warm, this ratio was only 1.5. Due to a lack of tests performed with negative temperature differences and high flow rates, no conclusion can yet be drawn for negative temperature differences between water and air. The thawing efficiency rate was nearly stable even if the flow increased. Further tests are needed to better understand this relation.

5. CONCLUSIONS AND PERSPECTIVES

In this paper a simple, low-cost, laboratory method is proposed to quantify the efficiency of conducto-convective heat transfer induced by sub-surface flow in the active layer in comparison with conductive heat transfer induced by air temperature. Two experiments were carried out involving thawing-cells filled with homogeneous frozen saturated soils. The first experiment submitted soils to thawing at controlled room temperature. The second experiment submitted the same type of soil to thawing at the same room temperature but with sub-surface flow. Soil temperatures were recorded during the entire test. Air temperature, soil temperature, flow and slope varied between tests. Four tests duplicates were experimented simultaneously and data recorded during the test were averaged to calculate the efficiency of conduction versus convection thawing rates.

Preliminary results showed that the methodology, based on key variables that affect heat transfer, was precise enough to evaluate and compare the efficiency of thawing by conduction versus convection under different scenarios. Our results suggest that when water temperatures were warmer than air temperatures, the thawing was significantly amplified. Future work should simulate higher flow rates to evaluate if there's a scaling effect on thawing efficiency (Veuille et al. 2015).

Heat balance at the convection and conduction thawing-cells scale will be achieved by a fully-coupled numerical thermal model calibrated against laboratory data. Such numerical model will be used to further examine the relation between sub-surface flow discharge, water temperature and air temperature.

ACKNOWLEDGEMENTS

We are grateful to G. Davesne, A. Prince, and M. Sliger for their help in the laboratory. Special thanks to Janice Festa from Transport Canada for making this project happen. This project was funded by Transport Canada, the Fonds de recherche du Québec – Nature et technologies (FRQNT), the Natural Sciences and Engineering Research Council of Canada (NSERC), the NSERC Discovery Frontiers grant 'Arctic Development and Adaptation to Permafrost in Transition' (ADAPT) and the Canada Foundation for Innovation.

REFERENCES

Andersland, O. B., Ladanyi, B. 2004. *Frozen Ground Engineering*, The American Society pf Civil Engineers & John Wiley & Sons, Inc., 2d Ed., USA.

ASTM, 2007a. Standard Test Method for Bulk Density (Unit Weight) and Voids in Aggregate, *ASTM C29 / C29M-07, ASTM International*, West Conshohocken, PA, USA.

ASTM, 2007b. Standard Test Method for Particle-Size Analysis of Soils. *ASTM Standard D-422*. ASTM International, West Conshohocken, PA, USA.

Bear, J.1972. *Dynamics of Fluids in Porous Media,* Dover publications Inc, New York, USA.

Bianchi, A., Fautrelle, Y., Etay, J. 2004. *Transferts Thermiques*, Presses Polytechniques et Universitaires Romandes, Lausanne, Switzerland.

Chassaing, P. 2010, *Mécanique des fluides, éléments d'un premier parcours*, Cépaduès, Toukourse, France.

Costard, F., Dupeyrat, L., Gautier, E., Carey-Gailhardis, E. 2003. Fluvial Thermal Erosion Investigations along a Rapidly Eroding River Bank: application to the Lena River (Central Siberia), *Earth Surface Processes and Landforms*, 28: 1349-1359. DOI: 10.1002/esp.592.

de Grandpré, I., Fortier, D., Stephani, E. 2012. Degradation of permafrost beneath a road embankment enhanced by advected in groundwater, 2012, *Canadian Journal of Earth Sciences*, 49: 953-962, DOI: 10.1139/e2012-018.

de Grandpré, I., Fortier, D**.**, Stephani, E. (2010) Impact of groundwater flow on permafrost degradation: implications for transportation infrastructures. *63rd Canadian Geotechnical Conference and the 6th Canadian Permafrost*, September 12-16, Calgary, Canada, p. 534-540.

Dupeyrat, L., Costard, F., Randriamazaoro, R., Gailhardis, E., Gautier, E., Fedorov, A. 2011. Effects of Ice Content on the Thermal Erosion of Permafrost: Implications for Coastal and Fluvial Erosion, *Permafrost and Periglacial Processes*, 22: 179-187. DOI: 10.1002/ppp.722.

Fortier, D., Allard, M., Shur, Y. 2007. Observation of rapid drainage system development by thermal erosion of ice wedges on Bylot Island, Canadian Arctic Archipelago, *Permafrost and Periglacial Processes*, 22(2): 179-187. DOI: 10.1002/ppp.595.

Fortier, D., Sliger, M., de Grandpré, I. 2014a. *Innovation en géotechnique du pergélisol : Évaluation d'une nouvelle technique pour la mesure de la capacité calorifique des sols*, Prepared for Transport Canada. Cold Regions Geomorphology and Geotechnical Laboratory (Geocryolab), University of Montreal, Montreal, Canada: 25 p.

Fortier, D., de Grandpré, I., Veuille, S., Verpaelst, M., Davesne, G., Grandmont, K. 2014b. *Impacts de l'écoulement souterrain sur la dégradation du pergélisol et la stabilité des routes construites sur remblai : Final Report.* Prepared for Transport Canada. Cold Regions Geomorphology and Geotechnical Laboratory (Geocryolab), University of Montreal, Montreal, Canada: 120 p.

Huysmans, M., Dessargues, A. 2005. Review of the use of Péclet numbers to determine the relative importance of advection and diffusion in low permeability environments, *Hydrogeology Journal*, 13: 895-904. DOI: 10.1007/s10040-004-0387-4.

Jorgenson, M., T., Romanovsky, V., Harden, J., Shur, Y., O'Donnell, J., Schur, E., A., G., Kanevskiy, M., Marchenko, S. 2010. Resilience and Vulnerability of Permafrost to Climate Warming, *Canadian Journal of Forest Research*, 40:1219-1236, DOI: 10.1139/X10-060.

Kane, D., L., Hinkel, K., M., Goering, D., J., Hinzman, L., D., Outlcalt, S., I. 2001. Non-conductive heat transfer associated with frozen soils, *Global and Planetary Change*, 29: 275-292. DOI: 10.1016/S0921-8181(01)00095-9.

Lunardini, V., J., Zisson, J., R., Yen, Y., C. 1986. *Experimental determination of heat transfer coefficients in water flowing over a horizontal ice sheet*, CRREL Report 86-3, US Army Cold Regions Research and Engineering Laboratory.

McKenzie, J., M., Voss, C., I. 2013. Permafrost thaw in a nested groundwater-flow system, *Hydrogeology Journal*, 21(1): 299-316. DOI: 10.1007/s10040-012-0942-3.

Overduin, P., P., Kane, D., L. 2006. Frost Boils and Soils Ice Content: Field Observations, *Permafrost and Periglacial Processes*, 17: 291-307. DOI: 10.1002/ppp.567.

Randriamazaoro, R., Dupeyrat, L., Costard, F., Gailhardis, E. C. 2007. Fluvial thermal erosion: heat balance integral method, *Earth Surface Processes and Landforms*, 32: 1828-1840. DOI: 10.1002/esp.1489.

Rowland, J., C., Travis, B., J., Wilson, C. J. 2011. The Role of advective heat transport in talik development beneath lakes and ponds in discontinuous permafrost, *Geophysical Research Letters*, 38*,* L17504. DOI: 10.1029/2011GL048497.

Shur, Y., Hinkel, K., M., Nelson, F., E. 2005. The transient layer: implications for geocryology and climate-change science, *Permafrost and Periglacial Process*, 16: 5-17. DOI: 10.1002/ppp.518.

van Everdingen, R. O. 1998. *Multi-Language Glossary of Permafrost and Related Ground-Ice Terms*, National Snow and Ice Data Center/World Data Center for Glaciology, Boulder, CO, USA.

Veuille, S., Verpaelst, M., Charbonneau, S., Grandmont, K., Fortier, D. 2015. *Quantifying heat advection by groundwater flow in the active layer: Laboratory simulations*. Joint Assembly AGC-AGU-AMC-UGC, 3-7 mai, Montreal, QC, Canada.

Williams, P. J., Smith, M. W., 1989, The Frozen Earth, Fundamentals of Geocryology, Cambridge University Press, Cambridge, USA.

Woo, M.-K., Kane, D. L., Carey, S., K., Yang, D. 2008. Progress in Permafrost hydrology in the new millennium, *Permafrost and Periglacial Processes*, 19: 237-254. DOI: 10.1002/ppp.613.

Zottola, J., Darrow, M., Daanen, R., Fortier, D., de Grandpré, I. 2012. Investigating the effect of groundwater flow on thermal stability of embankment over permafrost, *Cold Regions Engineering 2012*: 601-611. DOI: 10.1061/9780784412473.060.